Differentiation of Tuberculous from Pyogenic Brain Abscesses with In Vivo Proton MR Spectroscopy and Magnetization Transfer MR Imaging

Rakesh K. Gupta, Davender K. Vatsal, Nuzat Husain, Sanjeev Chawla, Kashi N. Prasad, Raja Roy, Rajesh Kumar, Deepak Jha and Mazhar Husain

AJNR Am J Neuroradiol 2001, 22 (8) 1503-1509
http://www.ajnr.org/content/22/8/1503

AJNR Am J Neuroradiol 22:1503–1509, September 2001

Differentiation of Tuberculous from Pyogenic Brain Abscesses with In Vivo Proton MR Spectroscopy and Magnetization Transfer MR Imaging

Rakesh K. Gupta, Davender K. Vatsal, Nuzat Husain, Sanjeev Chawla, Kashi N. Prasad, Raja Roy, Rajesh Kumar, Deepak Jha, and Mazhar Husain

BACKGROUND AND PURPOSE: **MR imaging features are nonspecific with respect to the causative organism for patients with brain abscesses. On the basis of the hypothesis that the biochemical environment depends on the infecting organism and might be different in tuberculous compared with pyogenic brain abscesses, this study attempted to determine whether pyogenic brain abscesses can be differentiated from tuberculous brain abscesses by use of magnetization transfer (MT) MR imaging and in vivo proton MR spectroscopy.**

METHODS: **Twenty-seven patients with a total of 33 pyogenic brain abscesses and three patients with a total of 12 tuberculous abscesses were evaluated with in vivo MR spectroscopy and MT MR imaging. The diagnosis in all cases was based on the culture of the causative organisms and histopathology whenever done as a part of clinical management.**

RESULTS: **All 27 patients with pyogenic brain abscesses had lipid and lactate levels of 1.3 ppm and amino acid levels of 0.9 ppm with or without the presence of succinate, acetate, alanine, and glycine, while the three patients with tuberculous abscesses showed only such lipid and lactate levels. The MT ratio from the wall of the pyogenic abscesses was significantly higher ($P < .001$) than that from the tuberculous abscess wall.**

CONCLUSION: **It might be possible to differentiate tuberculous abscesses from pyogenic abscesses by using MT MR imaging and in vivo MR spectroscopy, which could be of value in influencing the management of such cases.**

Tuberculous brain abscesses are extremely rare. They have been observed in immunocompromised as well as immunocompetent individuals (1, 2). The true tuberculous brain abscess, according to the criteria of Whitener (3), lies in macroscopic evidence of abscess formation within the brain parenchyma; histologic confirmation that the abscess wall is composed of vascular granulation tissue, containing acute and chronic inflammatory cells; and bacteriologic proof of the tuberculous origin. The neuroimaging study is usually nonspecific, and histopathologic examiniation/fix is the only definite method for diagnosing tuberculous brain abscesses.

A number of in vivo proton MR spectroscopy studies that are considered specific for pyogenic brain abscess and that help in differentiation of brain abscesses from glioblastoma multiforme have been done (4–9). Conventional MR imaging findings are nonspecific with respect to the causative agent for brain abscesses. It is not possible to differentiate a tuberculous from a pyogenic abscess on the basis of conventional MR features (10–12). Recently, magnetization transfer (MT) MR imaging was used for better tissue characterization in central nervous system tuberculosis (13). The MT ratio is influenced by the concentration of proteins and amino acids and may help in differentiation of tuberculous from pyogenic brain abscesses.

We describe the cases of three patients with multiple tuberculous brain abscesses in which the suggested diagnosis was based entirely on the combined use of MT MR imaging and in vivo MR spectroscopy. We also compare metabolite levels and MT ratios between pyogenic abscesses and tuberculous abscesses to determine any significant

Received February 6, 2001; accepted after revision March 27.

From the Departments of Radiology (R.K.G., S.C., R.K.) and Microbiology (K.N.P.), Sanjay Gandhi Post-Graduate Institute of Medical Sciences; the Departments of Neurosurgery (D.K.V., D.J., M.H.) and Pathology (N.H.), King George's Medical College; and the Regional Sophisticated Instrumentation Center, CDRI (R.R.), Lucknow, India.

D.K.V. and S.C. received financial assistance from the Council of Scientific and Industrial Research, New Delhi, India.

Address reprint requests to Rakesh K Gupta, Additional Professor, MR Section, Department of Radio-diagnosis, Sanjay Gandhi Post-Graduate Institute of Medical Sciences, Lucknow-226014, India.

Summary of results

Abscess	MT Ratio from the Wall*	Metabolites Seen on In Vivo MR Spectra	Metabolites Seen on Ex Vivo MR Spectra
Pyrogenic (n = 33)	25.56 ± 1.61	Succinate, leucine, isoleucine, valine, acetate, alanine, glycine, lipid and lactate	Succinate, leucine, isoleucine, valine, acetate, alanine, glycine, lipid and lactate
Tuberculous (n = 12)†	19.89 ± 1.55	Lipid, lactate, choline‡	Lipid, lactate, glycine, alanine

* $P < .001$ between MT ratios of the pyogenic and tuberculous wall.

† Spectral data obtained in five of 12 abscesses in three patients.

‡ Choline was seen as a contaminant from the wall of the abscess on spin-echo images (echo time, 135 ms).

difference. Our hypothesis was based on the fact that *Mycobacterium tuberculosis* is rich in lipids and produces fewer proteins and amino acids compared with the nontuberculous pyogenic bacteria that produce large amounts of hydrolytic enzymes, resulting in a high concentration of proteins and amino acids. The MT ratio is influenced by the concentration of proteins and amino acids; thus, MT ratios and MR spectra of the lesion could help in establishing the differentiation between a tuberculous abscess and pyogenic brain abscess.

Methods

We performed conventional MR imaging, in vivo MR spectroscopy, and MT MR imaging in 30 patients with brain abscesses during a 2-year period. Twenty-five age- and sex-matched control subjects also were studied with these techniques for comparison with patients' data with respect to MT ratios in different parenchymal locations and normal parenchymal spectral patterns. Three patients had 12 abscesses of tuberculous origin, and 27 patients had 33 abscesses of pyogenic origin (*Staphylococcus aureus* [n = 9], *Streptococcus faecalis* [n = 6], *Proteus mirabilis* [n = 2], *Klebsiella pneumoniae* [n = 2], *Escherichia coli* [n = 2], sterile [n = 6]). There were 21 male and nine female patients, and their ages ranged from 5 to 54 years. All 30 patients showed negative serology for human immunodeficiency virus infection. None of the patients with tuberculous brain abscess had any overt focus of infection in the lungs.

As a part of research protocol, all suspected brain abscesses were evaluated by in vivo MR spectroscopy and MT MR imaging. The diagnosis of pyogenic abscess was confirmed by aspiration and culture of the pus. In the remaining three patients with tuberculous brain abscesses, the diagnosis was confirmed by demonstration of acid-fast bacilli in the pus and the wall of the abscess cavity on Ziehl-Neelsen stain; nonspecific inflammation of the wall of the abscess cavity on histopathology; and subsequent culture of *M tuberculosis* from the pus.

MR imaging and spectroscopy were performed with a 1.5-T MR imaging system with a circularly polarized head coil. Each patient's head was fixed to prevent movement during and in between acquisition of images. Conventional spin-echo T1-weighted axial MR images at 1000/14/3 (TR/TE/excitations) and proton density– and T2-weighted axial MR images at 2200/12, 80/1 were obtained (section thickness, 5 mm; matrix size, 192 × 256; intersection gap, 0.5 mm). The pulse sequence used for MT contrast consisted of an off-resonance saturation pulse immediately before the 90-degree pulse (excitation pulse to saturate the magnetization of protons with restricted motion). The bandwidth of the saturation pulse was 250 Hz, and the frequency offset was 1.5 kHz. For T1-weighted MT images only a saturation pulse was added, and the other parameters were identical to those used for the conventional spin-echo T1-weighted images. The TR/TE parameters were so chosen as to minimize T1-weighted and T2-weighted effects. Postcontrast MT MR imaging also was performed in 29 patients, after intravenously injecting gadopentetate dimeglumine (0.1 mmol/kg). Conventional postcontrast spin-echo T1-weighted imaging was not done, as it has been shown that postcontrast T1-weighted MT MR images are better for visualization of the enhancing lesions (14, 15). Postcontrast study was not performed in one patient with tuberculous abscesses, as the patient did not cooperate for the injection of gadopentetate dimeglumine.

The MR images were evaluated and MT ratios were calculated independently by two authors (R.K.G., R.K.). Signal intensity from the same region of interest was measured from the conventional T1-weighted image without off-resonance pulse (S_0) and the MT MR image with off-resonance pulse (S_{mt}). The MT ratio was calculated by using the formula $(S_0 - S_{mt}/S_0) \times 100$ (16). The two authors did not disagree with respect to MT ratios. The regions of interest with a single pixel were obtained in different regions of the rim of the lesion, as suggested more clearly by T2-weighted images. Consistency and reliability of the measurements were confirmed by obtaining the values repeatedly. The MT ratios from the scalp fat, cerebrospinal fluid, and cortical and deep gray and white brain matter of 25 healthy control subjects between 5 and 50 years old were obtained. The regions of interest with a single pixel were obtained from the 10 regions of the cortices of the frontal, parietal, occipital, and temporal lobes or image-normal cortices per subject, in the 25 control subjects. Similarly, 10 regions of interest from the white matter were selected. For deep gray matter, regions of interest from the basal ganglia and thalami were included. Background noise was measured and divided by the square root of π.

→

FIG 1. Pyogenic brain abscess.

A, T2-weighted MR image through the temporal lobe shows a well-defined hyperintense lesion in the right temporal lobe with peripheral hypointense rim, perifocal edema, and mass effect on the ventricular system.

B, T1-weighted image shows the lesion as hypointense with isointense wall.

C, MT T1-weighted image shows minimal hyperintesity. The MT ratio from the wall is 31.25.

D, Postcontrast MT T1-weighted image shows enhancement of the rim of the lesion.

E and F, In vivo MR spectra obtained using STEAM (*E*) at 3000/20/30/128 (TR/TE/TM/excitations) and spin-echo (*F*) at 3000/135/128 (TR/TE/excitations) show presence of glycine (Gly) at 3.56 ppm; succinate (S) at 2.4 ppm; acetate (A) at 1.92 ppm; alanine (Al) at 1.5 ppm; lipid/lactate (Lip/L) at 1.3 ppm; and leucine, isoleucine, and valine (AA) at 0.9 ppm.

G and H, Ex vivo MR spectroscopy with single-pulse (*G*) and spin-echo (*H*) imaging confirm the assignments seen in vivo.

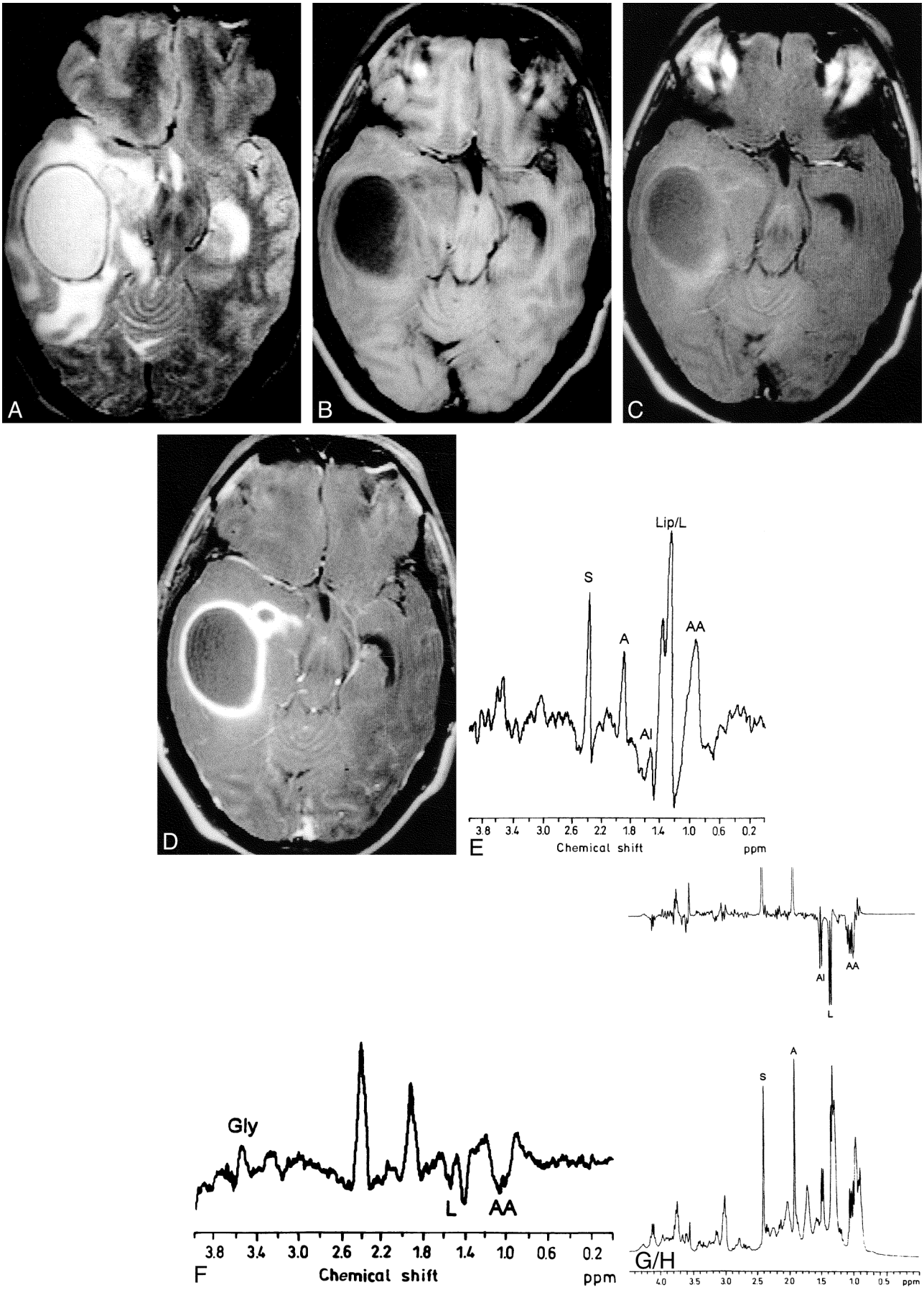
A
B
C
D
S
A
Al
Lip/L
AA
3.8 3.4 3.0 2.6 2.2 1.8 1.4 1.0 0.6 0.2
Chemical shift
ppm
E
Al
AA
L
Gly
L
AA
3.8 3.4 3.0 2.6 2.2 1.8 1.4 1.0 0.6 0.2
F
Chemical shift
ppm
S
A
G/H
4.0 3.5 3.0 2.5 2.0 1.5 1.0 0.5 ppm

Single-voxel MR spectroscopy was performed with stimulated echo acquisition mode (STEAM) (17) and/or spin-echo (18) localizing sequences with the following parameters: STEAM, 3000/20/30/128 (TR/TE/TM/excitations); spin echo, 3000/135/128 (TR/TE/excitations). The total time taken for imaging and spectroscopy ranged from 50 to 60 minutes. The assignment of metabolites was based on the literature (1–5). The voxel was set at 1.5 cm^3 for STEAM and 2.0 cm^3 for spin-echo sequences and placed in the center of the lesion, avoiding the wall of the abscess cavity if possible. Abscesses larger than 2 cm were selected for the in vivo MR spectroscopy. Only five of the 12 tuberculous abscesses fulfilled the size criteria for MR spectroscopy. The minimum voxel size of the spin-echo sequence available on our unit was 8 cm^3; hence, the wall of the lesion was included in spin-echo sequence acquisitions for three of these lesions.

Ex vivo MR spectroscopy of the aspirated pus was performed for all the samples of tuberculous abscess and for 15 of the 27 patients with pyogenic abscesses by using a 300-MHz Fourier transform nuclear MR spectrometer equipped with a 5-mm multinuclear inverse probe head with Z-shielded gradient. Typical parameters for obtaining the single-pulse spectrum were as follows: flip angle, 90 degrees; relaxation delay, 3.5 seconds, water presaturation power, 0.5 W; and acquisitions, 128. Spin-echo experiments were performed with an echo time of 80 ms. Standard correlated spectroscopy at 90 degrees was performed with water presaturation as used in the single-pulse experiments.

Results

All 25 healthy control subjects showed the following mean MT ratios: from cortical gray matter, 27.8 ± 0.55; deep gray matter, 24.81 ± 0.03; white matter, 36.3 ± 1.27; scalp fat, 8.4 ± 0.6; and cerebrospinal fluid, -3.68 ± 1.2 (19). MR spectroscopy showed major resonances of *N*-acetyl aspartate at 2.02 ppm, choline-containing compounds at 3.22 ppm, and total creatine at 3.02 ppm from different locations of the normal brain parenchyma.

A summary of the patient data is given in the Table. The mean MT ratio from the wall of the pyogenic brain abscesses measured 25.56 ± 1.61 ($n = 33$). MR spectroscopy in all these pyogenic abscesses showed the presence of lipid and lactate levels of 1.3 ppm and amino acids (leucine, isoleucine, and valine) at 0.9 ppm. In addition, succinate, 2.41 ppm ($n = 7$); acetate, 1.92 ppm ($n = 9$); alanine, 1.48 ppm ($n = 11$); and glycine, 3.56 ppm ($n = 15$) were seen (Fig 1).

Three patients had a total of 12 tuberculous abscesses. The mean MT ratio from the wall of the tuberculous abscesses measured 19.89 ± 1.55 and was found to be significantly lower ($P < .001$) than the wall of the pyogenic brain abscess, normal cortical and deep gray matter, and white matter. The MR spectroscopy of five of these 12 tuberculous abscesses showed lipid and lactate levels of 1.3 ppm; there was no evidence of amino acids at 0.9 ppm. In three of these five abscesses, choline-containing compounds (3.22 ppm) were observed during spin-echo imaging at an echo time of 135 milliseconds; this was because the minimal size of the voxel for spin-echo imaging at 135 milliseconds was 8 mL whereas that for STEAM at an echotime of 20 milliseconds was 3.37 mL, resulting in contamination from the wall of the abscess cavity (Fig 2). The results of in vivo study were confirmed by ex vivo MR spectroscopy in these three cases.

Discussion

The appearance of brain abscesses on MR imaging is nonspecific and does not suggest the specific etiologic agent responsible (10–12). Pyogenic brain abscesses on in vivo MR spectroscopy usually show the presence of amino acids at 0.9 ppm and lipid and lactate at 1.3 ppm, with or without the presence of acetate at 1.92 ppm and succinate at 2.4 ppm (Fig 1) (4–9). The amino acids are always observed in pyogenic brain abscesses, even when the patient is being treated with antibiotics and repeated aspiration (4, 5). The conventional MR imaging and MR spectroscopy in 27 patients had results consistent with those in the literature, and subsequently their cases could be confirmed as pyogenic abscesses. For three patients with imaging features of nonspecific abscesses, we observed only lipids and lactate on in vivo MR spectra, with no evidence of amino acids at 0.9 ppm (Fig 2) and, therefore, ruled out the possibility of pyogenic brain abscess. A spectral pattern similar to one observed in the present series, in cases of tuberculous abscess, has also been noted in patients with cystic glioblastoma multiforme (8, 9); however, on conventional MR images, the lesions in this study appeared like abscesses.

→

FIG 2. Multiple tuberculous abscesses.

T2-weighted (*A*), T1-weighted (*B*), MT T1-weighted (*C*), and postcontrast MT T1-weighted (*D*) images through the third ventricle show abscesses in the right caudate nucleus, right frontal and left periventricular regions. The lesions show hyperintense core and peripheral hypointense rim along with perifocal edema on T2-weighted image (*A*). On T1-weighted (*B*) and MT T1-weighted images (*C*), these lesions shown hypointense core with hyperintense rim, more clearly visible on MT T1-weighted images. Postcontrast MT T1-weighted image shows enhancement of the peripheral rim. Note an additional lesion (*arrow*) visible on *B, C,* and *D* that is not visible in *A.* The MT ratio from the wall of these three abscesses varied from 18.3 to 20.4. In MR spectroscopy done from the large right caudate nucleus lesion using STEAM at 20 (TE) with a voxel of 1.5 cm^3, only lipid and lactate (Lip/L) at 1.3 ppm are shown (*E*); on spin-echo spectrum at 135, phase reversal along with reduction in signal is seen (*F*). The presence of choline (Cho) in *F* results from the larger size of the voxel (2.0 cm^3) selected on spin-echo sequences that included the wall of the lesion. Ex vivo high-resolution, single-pulse (*G*) and spin-echo (*H*) proton MR spectroscopy at 80 ms confirm the presence of Lip/L with no evidence of choline. Histopathology of the wall (*I*) shows dense mixed inflammatory infiltrate; no epitheloid granulomas were seen (hematoxylin and eosin stain; original magnification, ×125). Ziehl-Neelsen stain of the wall (*J*) shows numerous acid-fast bacilli in clusters and individually (*arrows*) both in the intracellular and extracellular spaces (original magnification, × 1250).

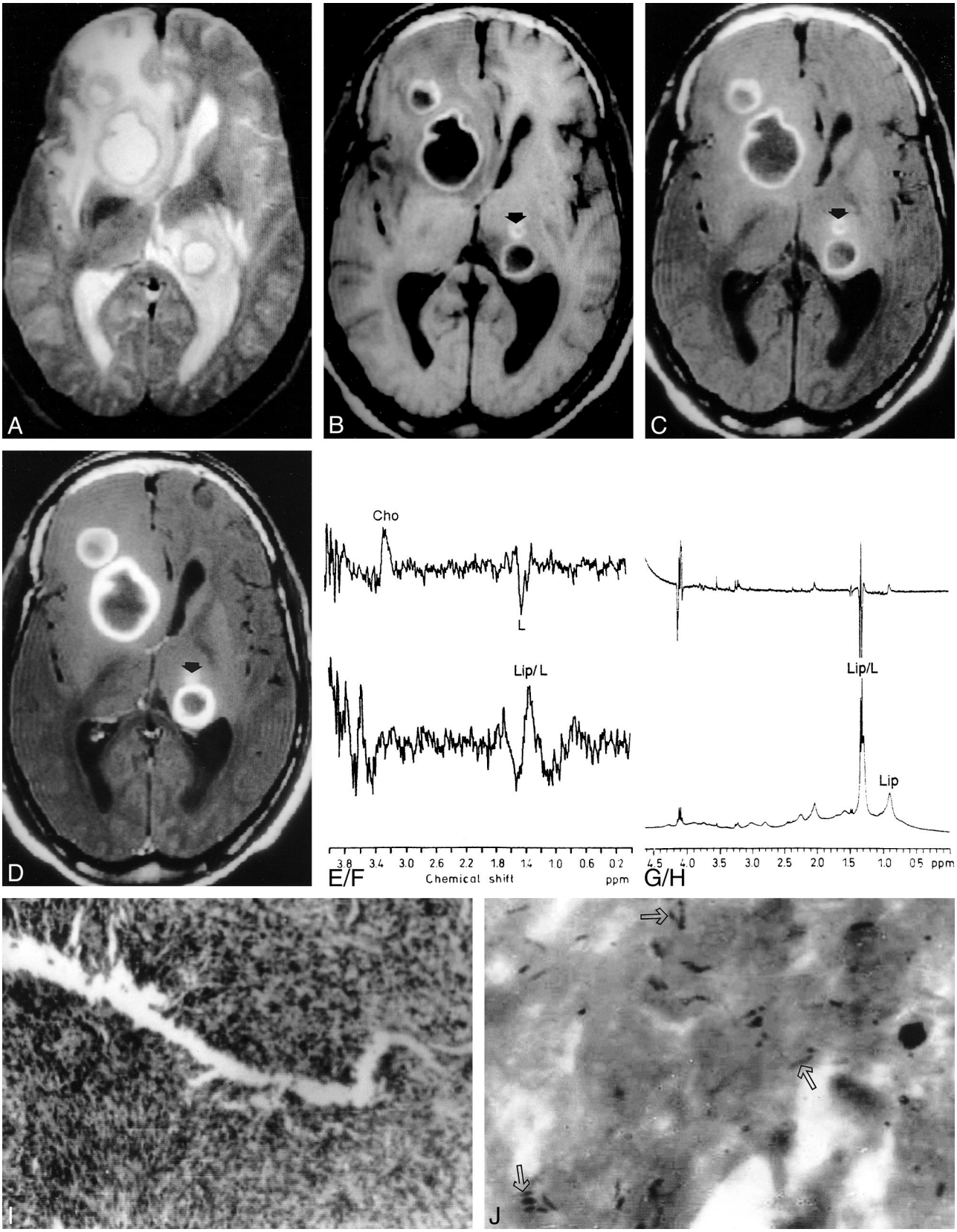
A
B
C
D
Cho
L
Lip/ L
3.8 3.4 3.0 2.6 2.2 1.8 1.4 1.0 0.6 0.2
Chemical shift
ppm
E/F
Lip/L
Lip
4.5 4.0 3.5 3.0 2.5 2.0 1.5 1.0 0.5 ppm
G/H
I
J

Pathologically, the pyogenic brain abscesses contain large amounts of neutrophils and proteins, which are released in the necrotic cavity. The breakdown of the neutrophils results in a release of a large amount of proteolytic enzymes that hydrolyze the proteins into amino acids (20). This is the reason for detecting the amino acids (leucine, isoleucine, and valine) at 0.9 ppm at in vivo MR spectroscopy in pyogenic brain abscesses. On the other hand, tuberculous abscesses teem with mycobacteria along with lymphocytes and a small number of neutrophils in the pus and necrotic brain tissue (3). The mycobacteria are predominantly composed of lipids (21). There is a relative lack of proteolytic enzymes in the tuberculous inflammatory exudates compared with pyogenic inflammation (22). The nonvisibility of the amino acids at 0.9 ppm in tuberculous abscesses probably stems from the presence of large amounts of mycobacteria and the lack of proteolytic enzymes, resulting in poor degradation of the proteins into amino acids. Presence of choline has been reported in benign inflammatory conditions, like xanthogranuloma, stroke, and other nonneoplastic lesions with dense inflammation (23, 24). Presence of choline in cystic lesions, like xanthogranuloma, and stroke are attributed to the inclusion of the cellular margins of these lesions in the voxel for MR spectroscopy (24). In this study, choline was observed in three tuberculous abscesses, which probably stems from the inclusion of cellular wall in the volume of interest on MR spectroscopy (Fig 2E and F). Absence of choline in tuberculous pus on ex vivo MR spectra (Fig 2G and H) further substantiates that the presence of choline in these three tuberculous abscesses resulted from the partial volume effect.

Tuberculomas usually appear hypointense on T2-weighted images and show lipid resonance at 1.3 ppm, 2.02 ppm, and 3.7 ppm at in vivo MR spectroscopy (11, 21, 25). This spectral pattern in a T2 hypointense lesion is considered characteristic of intracranial tuberculoma (21, 25). Tuberculomas must be differentiated from pseudoabscesses formed by the liquefaction of the caseous material in tuberculoma, which may appear similar to tuberculous abscess on conventional MR images. The wall of the tuberculoma appears hyperintense on MT T1-weighted images and characteristically shows the MT ratio from 18% to 22% (13). This hyperintense wall cannot be separated from edema on T2-weighted images (13, 26). In the present series, all 12 tuberculous abscesses in three patients showed a hyperintense center and hypointense peripheral rim on T2-weighted images. These lesions differed from tuberculoma on MT MR images. The hypointense peripheral rim on T2-weighted images for tuberculous brain abscess appeared hyperintense on MT T1- and T1-weighted images, whereas for tuberculomas, the T2 hypointensity is surrounded by a hyperintense rim on MT T1- and T1-weighted images, not visible on T2-weighted images as this layer merges with edema (13, 27). The T2, MT T1, and histopathologic correlation in tuberculoma has shown that the MT T1 hyperintense rim is composed of granuloma, cellular infiltrates, and gliosis (27). It is interesting to note that the MT ratio of the cellular rim of tuberculoma having granulomas has matched the nonspecific cellular reaction of the tuberculous abscess containing a large number of intracellular and extracellular *M tuberculosis*. The wall of granuloma contains the breakdown products of the tubercle bacilli (21, 25). The cellular rim of tuberculoma and wall of tuberculous abscess are rich in lipids and, hence, show MT ratios in the same range.

The MT ratio of tuberculous meningitis has been described as being significantly lower than that of pyogenic and fungal meningitis (13). This has been explained by the fact that pyogenic and fungal meningitis elicit large amounts of amino acids and protein, while tuberculous meningitis shows large amounts of lipids with small amounts of amino acids. The MT ratio from the wall of the pyogenic abscess was significantly higher than that from the wall of the tuberculous abscess. The wall of the tuberculous abscess contains large numbers of mycobacteria inside and outside the cells, along with chronic nonspecific inflammatory cells (Fig 2I and J), while the wall of the pyogenic abscess contains inflammatory cells. The presence of large numbers of tubercle bacilli is probably responsible for the lower MT ratio in tuberculous compared with pyogenic brain abscesses.

The diagnosis of tuberculous brain abscess is usually suspected in immunocompromised patients with or without human immunodeficiency virus infection or in an immunocompetent patient from an endemic region with a pulmonary focus of infection. This pulmonary focus of infection is usually present in only 30% of cases (26). In the absence of an extracranial focus of infection, it might be very difficult to suspect tuberculous brain abscess on the basis of clinical and imaging features, as these are nonspecific. In the present study, there were no detectable stigmas of tuberculosis elsewhere in the body and conventional spin-echo MR imaging was unhelpful in detecting the offending organism. Diagnosis in these cases was objectively suggested on the basis of MT MR imaging and spectroscopy findings.

Differentiation of tuberculous brain abscess from pyogenic abscess is important for management. Combined medical and surgical treatment (repeated aspirations) is recommended for the care of patients with pyogenic brain abscess (28, 29), whereas surgical excision and antituberculous treatment are the norms for managing these tuberculous brain abscess (30–32). In the present series, seven of 12 tuberculous abscesses were excised, as these patients were showing clinical deterioration while undergoing antituberculous treatment; pyogenic abscesses were managed with repeated aspiration and antibiotic therapy.

Conclusion

Tuberculous brain abscesses show significantly lower MT ratios compared with those of pyogenic abscesses with no evidence of amino acids at in vivo MR spectroscopy, a spectral hallmark of the pyogenic abscess. We believe that, when MT MR imaging is combined with in vivo MR spectroscopy, it might be possible to differentiate tuberculous brain abscesses from pyogenic brain abscesses, as both appear similar on conventional MR images. This differentiation would allow for better management of these cases.

Acknowledgments

Davender K. Vatsal and Sanjeev Chawla acknowledge the financial assistance of the Council of Scientific and Industrial Research, New Delhi, India.

References

1. Farrar DJ, Flanigan TP, Gordon NM, Gold RL, Rich JD. **Tuberculous brain abscess in a patient with HIV infection: case report and review.** *Am J Med* 1997;102:297–301
2. Schoeman JF, Morkel A, Seifart HI, et al. **Massive posterior fossa tuberculous abscess developing in a young child treated for miliary tuberculosis.** *Pediatr Neurosurg* 1998;29:64–68
3. Whitener DR. **Tuberculous brain abscess.** *Arch Neurol* 1978;35: 148–155
4. Dev R, Gupta RK, Poptani H, Roy R, Sharma S, Husain M. **Role of in vivo proton magnetic resonance spectroscopy in diagnosis and management of brain abscesses.** *Neurosurgery* 1998;42: 37–43
5. Grand S, Passaro G, Ziegler A, et al. **Necrotic tumor versus brain abscess: importance of amino acids detected at 1H MR spectroscopy—initial results.** *Radiology* 1999;213:785–793
6. Poptani H, Gupta RK, Jain VK, Roy R, Pandey R. **Cystic intracranial mass lesion: possible role of in vivo MR spectroscopy in its differential diagnosis.** *Magn Reson Imaging* 1995;13: 1019–1029
7. Poptani H, Gupta RK, Roy R, Pandey R, Jain VK, Chhabra DK. **Characterization of intracranial mass lesions with in vivo MR spectroscopy.** *Am J Neuroradiol* 1995;16:1593–1603
8. Kim SH, Chang KH, Song IC, et al. **Brain abscess and brain tumor: discrimination with in vivo H-1 MR spectroscopy.** *Radiology* 1997;204:239–245
9. Chang KH, Song IC, Kim H, et al. **In vivo single voxel proton MR spectroscopy in intracranial cystic masses.** *AJNR Am J Neuroradiol* 1998;19:401–405
10. Haimes AB, Zimmerman RD, Morgello S, et al. **MR imaging of brain abscess.** *AJNR Am J Neuroradiol* 1989;10:279–291
11. Jinkins JR, Gupta R, Chang KH, Carbajal-Rodriguéz J. **MR imaging of central nervous tuberculosis.** *Radiol Clin North Am* 1995;33:771–786
12. Bowen BC, Post MJD. **Intracranial infection.** In: Atlas SW, ed. *Magnetic Resonance Imaging of the Brain and Spine.* New York, NY: Raven Press; 1997: 501–538
13. Gupta RK, Kathuria M, Pradhan S. **Magnetization transfer MR imaging in central nervous tuberculosis.** *AJNR Am J Neuroradiol* 1999;20:867–875
14. Hametaka G, Korogi Y, Sakamato Y, et al. **Value of magnetization transfer contrast in intracranial enhancing and non-enhancing lesions with paramagnetic contrast agents.** *Radiat Med* 1997;15:295–303
15. Fineli DA, Hursr GC, Gullapalli RP. **T1- weighted three- dimensional magnetization transfer magnetic resonance of the brain improved lesion contrast enhancement.** *AJNR Am J Neuroradiol* 1998;19:59–64
16. Dousset V, Grossman RI, Ramer KN, et al. **Experimental allergic encephalomyelitis and multiple sclerosis lesion characterization with magnetization transfer imaging.** *Radiology* 1992;182: 483–491
17. Frahm J, Merboldt KD, Hanicke W. **Localized proton spectroscopy using stimulated echoes.** *J Magn Reson* 1987;72:502–508
18. Bottomley PA. **Selective volume method for performing localized NMR spectroscopy.** US patent 4 480 228. 1984
19. Kathuria MK, Gupta RK, Roy R, Gaur V, Husain N, Pradhan S. **Measurement of magnetization transfer in different stages of neurocysticercosis.** *J Magn Reson Imaging* 1998;8:473–479
20. Mendz GL, McCall MN, Kuchel PW. **Identification of methyl resonances in the 1H NMR spectrum of incubated blood cell lysate.** *J Biol Chem* 1989;264:2100–2107
21. Gupta RK, Roy R, Poptani H, et al. **Finger printing of *Mycobacterium tuberculosis* in intracranial tuberculomas using in vivo, ex vivo and in vitro proton spectroscopy.** *Magn Reson Med* 1996;36:829–833
22. Chapman M, Murray RO, Stoker DJ. **Tuberculosis of the bones and joints.** *Semin Roentgenol* 1979;14:266–282
23. Krouwer HGJ, Kim TA, Rand SD, et al. **Single voxel proton MR spectroscopy of nonneoplastic brain lesions suggestive of neoplasm.** *AJNR Am J Neuroradiol* 1998;19:1695–1703
24. Dave AS, Gupta RK, Roy R, et al. **Prospective evaluation of in vivo proton MR spectroscopy in differentiation of similar appearing intracranial cystic lesions.** *Magn Reson Imaging.* 2001; 19:103–110
25. Gupta RK, Roy R. **MR imaging and spectroscopy of intracranial tuberculomas.** *Curr Sci* 1999;76:783–788
26. Barnes PF, Bloch AB, Davidson PT, Snider DE. **Tuberculosis in patients with human immunodeficiency virus infection.** *N Engl J Med* 1991;324:1644–1650
27. Gupta RK, Husain N, Kathuria MK, Datta S, Rathore RKS, Husain M. **Magnetization transfer MR imaging is more close to histopathology than conventional MR imaging in intracranial tuberculomas.** Proceedings of the Eighth Meeting of the International Society for Magnetic Resonance in Medicine. Berkeley, Calif: International Society for Magnetic Resonance in Medicine, 2000;1105
28. Mamelak AN, Mampalam TJ, Obana WG, Rosenblum ML. **Improved management of multiple brain abscesses: a combined surgical and medical approach.** *Neurosurgery* 1995;36:76–86
29. Osenbach RK, Loftus CM. **Diagnosis and management of brain abscess.** *Neurosurg Clin North Am* 1992;3:403–420
30. Bannister CM. **A tuberculosis abscess of the brain: case report.** *Neurosurgery* 1970;33:203–206
31. Prakash B, Mehta G, Gondal R, Kumar S, Malhotra V. **Tuberculous abscesses of the brain stem.** *Surg Neurol* 1989;32: 445–448
32. Mohanty A, Venkatarama SK, Vasudev MK, Khanna N, Anandh B. **Role of stereotactic aspiration in the management of tuberculous brain abscess.** *Surg Neurol* 1999;51:443–447